Soil Biology and Biochemistry 203 (2025) 109740

Contents lists available at ScienceDirect

Soil Biology and Biochemistry

journal homepage: www.elsevier.com/locate/soilbio

Microbial carbon use efficiency of mineral-associated organic matter is related to its desorbability

Alexander Konrad [a,*], Diana Hofmann [b], Jan Siemens [a], Kenton P. Stutz [c], Friederike Lang [c], Ines Mulder [a,d]

[a] Institute of Soil Science and Soil Conservation, iFZ Research Center for Biosystems, Land Use and Nutrition, Justus Liebig University Giessen, Heinrich Buff Ring 26-32, 35390, Giessen, Germany
[b] Institute of Bio- and Geosciences, Agrosphere (IBG-3), Forschungszentrum Jülich, Wilhelm-Johnen-Str., 52425, Jülich, Germany
[c] Soil Ecology, Institute of Forest Sciences, University of Freiburg, Bertoldstraße 17, 79098, Freiburg, Germany
[d] Institute of Geography, Soil Sciences and Soil Resources, Ruhr University Bochum, Universitätsstr. 150, 44801, Bochum, Germany

ARTICLE INFO

Keywords:
Carbon use efficiency
Mineral-associated organic matter
Sorption
Desorption
Carbon cycling
Priming
Carbon sequestration

ABSTRACT

Interactions between organic substances, minerals, and microorganisms are crucial for organic carbon (OC) stabilization in soil. We hypothesized that thresholds of sorption strength (described by the sorption coefficient of the Freundlich isotherms) and desorbability (i.e., the ratio of the amount desorbed to the amount sorbed) of organic monomers control the extent of their microbial processing.

Freundlich sorption isotherms and desorbability of uniformly ^{14}C-labeled glucose, acetylglucosamine, phenylalanine, salicylic acid, and citric acid onto goethite, kaolinite, and illite were studied in batch experiments. Monomers adsorbed to minerals were mixed with loamy and sandy arable topsoil and incubated at 25 °C. Mineralization of mineral-adsorbed monomers was observed over three weeks, after which the assimilation into microbial biomass, and the ^{14}C remaining in soil were quantified. Subsequently, the mineralization of incubated soils was observed for additional three weeks after glucose priming.

The adsorption of carboxylic acids onto minerals exceeded that of (amino) sugars and phenylalanine, with the overall highest amounts both adsorbed and retained after desorption with water for goethite. Assimilation of monomer ^{14}C into microbial biomass and the microbial carbon use efficiency (CUE) of mineral-adsorbed monomers in both soils increased linearly with the monomer desorbability from mineral phases. Furthermore, the CUEs of monomers adsorbed to goethite were lower than those of the same monomers adsorbed to clay minerals. In terms of total amount of carbon retained in the soil, carboxylic acids adsorbed on goethite showed highest values, emphasizing the significance of oxides for the stabilization of OC within soils. Priming of incubated soil with non-labeled glucose caused an additional mineralization of monomer-C, with the priming effect decreasing from goethite to clay minerals.

We conclude that sorption strength and desorbability shape microbial utilization of mineral-bound organic compounds, but no universal thresholds determine bio-accessibility of sorbed organic compounds.

1. Introduction

Soils represent the largest terrestrial carbon (C) reservoir. Sequestration of organic C (OC) in soils plays a significant role in global C cycling, though the contribution of regulating factors remain uncertain (Georgiou et al., 2022). In the past decade, theories that emphasize the relevance of recalcitrance of biomolecules for OC sequestration have been superseded by concepts that stress the occlusion of OC in soil aggregates and sorption of OC to mineral surfaces (e.g. Lehmann and Kleber, 2015). These concepts also include the pathways by which OC enters the soil (Sokol et al., 2019) with subsequent microbial processing of diverse plant litter for stabilizing OC (Cotrufo et al., 2013; Lehmann et al., 2020).

Sorption to minerals slows down the mineralization of OC as demonstrated in laboratory experiments (Jones and Edwards, 1998; Kalbitz et al., 2005; Mikutta et al., 2007; Saidy et al., 2015) and the age distributions of OC across soil depths and fractions (Kleber et al., 2005; Schrumpf et al., 2013; Spielvogel et al., 2008). The capacity of minerals

* Corresponding author.
E-mail address: alexander.konrad@umwelt.uni-giessen.de (A. Konrad).

https://doi.org/10.1016/j.soilbio.2025.109740
Received 30 August 2024; Received in revised form 19 December 2024; Accepted 6 February 2025
Available online 7 February 2025

to bind OC as mineral-associated OC (MAOC) differs between 1:1 clay minerals with low sorption capacity, 2:1 clay minerals with high sorption capacity, and iron oxyhydroxides (Fe oxides) with exceptional sorption capacity due to their net positive surface charges in acidic and neutral soils (Feng et al., 2013; Gao et al., 2018; Georgiou et al., 2022; Saidy et al., 2013). The sorbate matters as well: smaller and more functionalized compounds such as deprotonated carboxylic acids adsorb more strongly and are more efficiently preserved in soils than sugars and neutral amino acids (Jones and Edwards, 1998; Yeasmin et al., 2014).

Aside sorption, biotic factors play a pivotal role in soil C cycling. Approximately half of all OC in arable soil exhibits molecular signatures of microbial origin (Angst et al., 2021). Models predicting soil OC cycling attempt to account for this by integrating microbial carbon use efficiency (CUE) which is defined as the ratio of OC remaining in the microbial biomass to the OC consumed (Sulman et al., 2014; Wang et al., 2013). In soil, CUE of the same molecule can exhibit considerable variation (Brown and Jones, 2024) due to microorganisms optimizing their fitness (Schimel, 2023). Minerals can affect CUE since they act as both microbial habitats as well as sinks for OC and nutrients like phosphorus (P)-containing organic and inorganic compounds (Kandeler et al., 2019; Spohn, 2024; Uroz et al., 2015).

Organic C translocated in the soil solution or released by roots into the rhizosphere—a zone of high microbial activity (Berendsen et al., 2012)—can enhance mineralization of mineral-associated organic carbon (MAOC) through a process known as “priming” (Jilling et al., 2021). Sugars, like glucose, are among the most abundant root exudates, play a key role in fueling the soil microbiome (Gunina and Kuzyakov, 2015; Hütsch et al., 2002). The glucose-induced priming effect on sorbed small organic molecules with different functional groups has been minimally investigated so far.

Regardless of priming effects, microbial processing of sorbed compounds would necessarily depend on desorbability (e.g., the ratio of the amount desorbed to the amount sorbed). However, the interaction between sorption strength (approximated by the sorption coefficient from Freundlich isotherms), desorbability, and microbial processing has yet to be quantified. We hypothesize that (1) the sorption strength and desorbability of monomers control microbial processing, with thresholds of sorption strength and desorbability determining the quantity of microbial processing, (2) in addition to the biochemical processes involved in metabolism, adsorption and release of monomers from mineral surfaces, as well as soil properties, affect microbial CUE, and (3) the addition of glucose increases the mineralization of adsorbed monomers due to priming, and the priming-induced mineralization increases with the strength of sorption and thus retention of OC.

These hypotheses were tested in sorption-desorption experiments with uniformly ^{14}C-labeled monomers and kaolinite (1:1 clay mineral), illite (2:1 clay mineral), and goethite (Fe-(oxyhydr)oxide), combined with incubation experiments of mineral-monomer associations in two arable topsoils with differing clay content. Kaolinite, illite, and goethite were selected as they represent distinct mineral classes with unique sorption characteristics. Kaolinite has limited cation exchange capacity but exposes hydroxyl groups, influencing adsorption through hydrogen bonding. Illite, with a higher cation exchange capacity, supports various interactions (Sposito, 2020), while goethite’s high surface charge and hydroxyl groups allow for strong ligand exchange (Cornell and Schwertmann, 2003). Glucose (sugar), acetylglucosamine (amino sugar), phenylalanine (amino acid), and carboxylic acids (salicylic and citric acid) were chosen as model compounds of organic monomers due to their ubiquity in soils and range of functional groups relevant to microbial processing (Kleber et al., 2021). Sugars tend to interact through weak adsorption, amino acids through polar and hydrophobic interactions, and carboxylic acids through ligand bonding (Jones and Edwards, 1998; Yeasmin et al., 2014). To assess microbial P limitation from mineral additions, particularly goethite, phosphate levels in the soil solution were measured after three weeks of incubation. Additionally, the incubation experiment for glucose adsorbed to goethite in the clayey soil was repeated after pre-saturating the goethite with phosphate to test whether alleviating potential P limitations would increase microbial carbon use efficiency for glucose. Soils were further treated with non-labeled glucose after incubating for three weeks and mineralization of monomer-C was quantified for additional three weeks to assess whether mineral-adsorbed monomers were susceptible to priming. Together, these combinations of minerals and monomers allowed us to explore a broad range of sorption behaviors and their effects on microbial processing, offering insights into how mineral composition influences the stability and bioavailability of mineral-adsorbed OC in soils.

2. Materials and methods

2.1. Materials and chemical reagents

Non-labeled chemicals with purities >99% were procured from Sigma-Aldrich (Darmstadt, Germany). Polyethylensulfone syringe filters with pore sizes of <220 nm and <450 nm were sourced from VWR International GmbH (Darmstadt, Germany). Uniformly ^{14}C labeled D-glucose, N-acetyl-D-glucosamine, L-phenylalanine, salicylic acid, and citric acid were procured from American Radiolabeled Chemicals (St. Louis, Missouri, USA). Ultra-pure water (18.2 MΩ, <2 ppb TOC) was obtained from a Purelab Flex 2 Water Purification System (Veolia Water Solutions and Technologies, Buckinghamshire, Unted Kingdom).

2.2. Preparation of model minerals

Two phyllosilicates, kaolinite (Quarzwerke GmbH, Frechen, Germany) and illite (Inter-ILI. Engineering Co. Ltd., Kosd, Hungary), as well as a self-synthesized goethite, were selected as sorbents. The clay minerals were freed from carbonates, iron oxides, and OC in accordance with the methodology outlined by Tributh and Lagaly (1986). Subsequently, the pH was adjusted to 10 using sodium carbonate, and the clay size fraction <2 μm was separated by sedimentation based on Stokes’ law. The samples were transferred into cellulose acetate tubing (Spectra/Por 2 RC Tubing, with a molecular weight cut-off of 12–14 kDa, Spectrum Laboratories, Inc., Rancho Dominguez, California, USA) and placed in buckets filled with deionized water for dialysis to remove salts. The deionized water was replaced frequently until the electrical conductivity of the suspension reached values below 10 μS cm^{-1}. Goethite was synthesized according to the methodology described by (Dultz et al., 2019). In brief, 10 M NaOH was added at a flow rate of 1 ml min^{-1} to a constantly stirred 0.5 M $FeCl_3$ solution, up to a pH of 12. Subsequently, the suspension was stored at 4 °C for 68 days, after which the pH was adjusted to pH 6 with 0.1 M HCl. The suspension was then dialyzed and freeze-dried analogously to the procedure for the clay minerals. Purified clay minerals and self-synthesized goethite were ground with a mortar and pestle and characterized by powder X-ray diffraction analysis (Empyrean, Malvern PANalytical B.V., Malvern, United Kingdom) to ascertain their purity (Supplementary material S1). Specific surface areas (SSA) were measured by N_2 adsorption using the Brunauer-Emmett-Teller method on a Quantachrome Quadrasorb evo (3P Instruments GmbH & Co. KG, Odelzhausen, Germany), showing SSA of 92.5, 17.2 and 43.7 m^2 g^{-1} for goethite, kaolinite and illite, respectively. Scanning electron microscopy images of the minerals were obtained using a GeminiSEM 560 (Carl Zeiss Microscopy Deutschland GmbH, Oberkochen, Germany) (Supplementary material S1).

2.3. Measurement of radioactivity

Quantification of ^{14}C was conducted for both the sorption-desorption batch study and the soil incubation experiments (a graphical overview on the experimental setup can be found in the Supplementary material S2). The radioactivity was measured using a daily calibrated TriCarb 3300 (PerkinElmer, Inc., Shelton, Connecticut, USA) liquid scintillation counter (LSC). All liquid samples (sodium hydroxide solutions as CO_2

sinks, soil extracts) were mixed with 10 mL of Ultima Gold XR scintillation cocktail (PerkinElmer, Inc., Shelton, Connecticut, USA) and vigorously shaken prior to scintillation counting. Solid samples (e.g. minerals and soils) were incinerated using a Hidex OX 600 oxidizer (Hidex Oy, Turku, Finland) using Oxysolve C-400 scintillation cocktail (Zinsser Analytic, Frankfurt, Germany) for subsequent LSC measurements. The oxidizer results were corrected for ^{14}C recovery rates. It has been recently reported that $^{14}CO_2$, trapped in NaOH, will degas from the lye-cocktail mixture over time, depending on CO_2 saturation, used scintillation cocktail and the time evolved before measurement (Boos et al., 2022, 2023). We accounted for this phenomenon by repeated measurements of same CO_2-samples and corrected the mineralization data with the resulting calibration curve (Supplementary material S3).

2.4. Sorption isotherms and desorbability

Sodium azide solutions were used at 0.01 M as background electrolyte for suspensions and solutions to prevent microbial action (Cabrol et al., 2017). Minerals were suspended at concentrations of 40.80 g L^{-1}, 40.13 g L^{-1} and 9.28 g L^{-1} for kaolinite, illite and goethite, respectively. The pH of the suspensions was adjusted to 5.5 using NaOH and HCl. Solutions of ^{14}C-labeled monomers (4000 Bq mL^{-1}) were prepared at concentrations of 0.02, 0.1, 0.2, 0.5, 1.0 and 2.0 mM, set to pH 5.5 and filtered through <0.22 μm polyether sulfone filters for sterilization. Batch sorption studies were conducted in triplicates in 1.5 mL polypropylene tubes (Sarstedt AG &Co., Nümbrecht, Germany) by mixing 0.5 mL of mineral suspension with 0.5 mL of monomer solution for all concentrations. Thus, monomer concentrations inside the tubes ranged between 0.01 and 1.0 mM and were corrected for mineral volume displacing solution. Tubes containing 0.5 mL 0.01 M NaN_3 and 0.5 mL ^{14}C-labeled monomer solution were prepared for the second lowest and second highest monomer concentration to check for adsorption on surface of the tubes and microbial processing of monomer in accordance to OECD guideline 106 (OECD, 2000). Tubes were shaken for 16 h at 1500 rpm at 25 °C (neoMix, neoLab Migge GmbH, Heidelberg, Germany) in the dark, centrifuged for 10 min at 17,000 g so that 920 μL of the supernatant could be retrieved for scintillation counting.

Reversibility of monomer adsorption for each model compound was determined at second lowest and second highest concentration using a two-step desorption procedure. Minerals from the batch sorption study were resuspended in 920 μL of fresh 0.01 M NaN_3 and shaken for 1 h at 1500 rpm in the dark, followed by centrifugation and removal of 920 μL of supernatant, analogous to the procedure of the sorption study. The desorption step was repeated with pH 5.5 adjusted NaH_2PO_4 at a concentration of 0.1 M as competing anion for 1 h. Minerals used for the desorption experiments were resuspended in NaN_3 and oxidized to check activity balance. At highest concentrations, analogous sorption experiments with non-labeled solutions were performed and supernatant checked for cations using optical emission spectroscopy with inductively coupled plasma (ICP-OES) (Agilent 720 ICP-OES ES, Agilent Technologies Inc., Santa Clara, USA) to exclude mineral dissolution in the presence of organic molecules.

2.5. Incubation

Minerals were sterilized by γ-irradiation of 10 kGy with a ^{60}Co source (Dalkmann et al., 2014), subsequently suspended in a sterile-filtered 0.01 M NaCl solution and set to pH 5.5. Sterile mineral suspensions and sterile-filtered ^{14}C-monomer solutions at pH 5.5 were added at concentrations matching those of the second lowest concentration of the sorption study into 50 mL PP centrifuge tubes and shaken end-over-end for 16 h at 25 °C. This concentration was chosen in order to avoid a saturation of sorption sites while loading the minerals with monomers (which would be a concern at higher concentrations), as well as the antimicrobial effects of salicylic and citric acids (Fang et al., 2020; Khan et al., 2020). The resulting suspensions were then centrifuged at 4.000 g for 2 h, the complete supernatant discarded. The mineral pellet was centrifuged again, and excess solution removed. The minerals were freeze-dried and ground, aliquots of the minerals were combusted. Farmyard manure-fertilized, air-dried arable topsoils sieved at < 2 mm from 2 to 20 cm soil depth were collected from two long-term field experiments in Germany as disturbed soil samples and used for incubation experiments according to OECD test no. 307 (OECD, 2002). Dikopshof soil is a moderately aggregated Haplic Luvisol, while the Thyrow soil is a weakly aggregated Haplic Retisol (Table 1). A complete description including microbial and mineralogical data is available in the publication by Lorenz et al. (2024).

The soils were pre-incubated at 60% water holding capacity for 10 days at 25 °C in the dark. The amount of mineral with adsorbed monomers added to the soils was chosen in a way that the soil mineral composition was changed as little as possible, while providing sufficient ^{14}C for detection. For each treatment (soil x mineral x monomer), 56 g of pre-incubated soil and 240 mg of ^{14}C-loaded, freeze-dried goethite, or 300 mg of ^{14}C-loaded clay mineral were carefully admixed with a spatula for 10 min. Duran flasks with a volume of 250 mL (SCHOTT AG, Mainz, Germany) were modified by the addition of a bent wire fixed to the cap of the flask, which held a standard 20 mL PP LSC vial filled with 1 mL of 1 M NaOH. Each mineral-admixed, pre-incubated soil (equal to 14 g of air-dry soil) was filled in triplicate into the modified glass flasks, resulting in a 1-cm-thick soil layer at the bottom of the flasks. To quantify exactly the added radioactivity and check for initial mineralization until airtight sealing of the incubation vessels after 20 min of mineral addition, three aliquots of 0.5 g each were taken out of each flask, ethanol was added in excess, the soil was dried, and ^{14}C activity was measured. The flasks were incubated at 25 °C in a circulating air incubation cabinet in the dark. Sodium hydroxide in the alkali traps was replaced frequently and $^{14}CO_2$ measured. To counteract the loss of water during sample collection and the hydrophilic nature of NaOH, strips of humid paper tissues of 3 × 7 cm were added hanging into the incubation flasks.

Water-extractable ^{14}C, microbial biomass ^{14}C, and bulk soil ^{14}C were determined after three weeks of incubation using three aliquots of 0.5 g of incubated soil from each replicate. The water content of the aliquots utilized for the bulk soil ^{14}C measurements was analyzed using a HB43–S halogen moisture analyzer (Mettler Toledo Inc., Columbus, USA), which demonstrated comparable water contents to those observed at the outset of the experiment, with a mean of 60 ± 4% WHC. The remaining aliquots were extracted using a chloroform fumigation extraction (CFE), as described by Vance et al. (1987) and modified by Murage and Voroney (2007) in 15 mL centrifuge tubes. Briefly, one aliquot from each incubation replicate was fumigated with chloroform for 16 h, afterwards extracted with 2.5 mL of 2 M KCl for 90 min shaking end-over-end. The remaining non-fumigated aliquot was directly, analogously extracted. All tubes were subsequently centrifuged, and the supernatant filtered. The ^{14}C content of the extracts was measured, with the difference between fumigated and non-fumigated extracts yielding microbial biomass ^{14}C. The non-fumigated extracts were used as a proxy for water-extractable organic ^{14}C ($WEO^{14}C$). Microbial CUE was calculated as the percentage of ^{14}C assimilated into microbial biomass to ^{14}C microbially processed (^{14}C assimilated + ^{14}C mineralized). Furthermore, the phosphate concentrations in non-fumigated extracts were quantified photometrically (Genesys 150, ThermoFisher Scientific Inc., Waltham, Massachusetts, USA) as phosphomolybdate complexes with malachite green at 660 nm (Van Veldhoven and Mannaerts, 1987).

After three weeks of incubation, non-labeled glucose solutions (similar to 0.1% of the soil organic carbon content) were added and admixed carefully with a spatula to the remaining mineral-amended incubation flask replicates (Blagodatskaya et al., 2009), resulting in a 5- to 10-fold higher OC input into the soil compared to the average daily root exudation (Kuzyakov and Domanski, 2000). The incubation period was extended for further three weeks, during which time the evolution of $^{14}CO_2$ was more frequently measured. At the experimental endpoint,

Table 1
Total organic carbon (TOC), total nitrogen (TN), TOC/TN ratio (C/N), total soil phosphorus (P), oxalate-extractable iron (Fe_O), dithionite-extractable iron (Fe_d), and basal respiration of the arable topsoils Dikopshof and Thyrow.

Site	Soil group	TOC [%]	TN [%]	C/N	P [mg kg^{-1}]	Fe_o [g kg^{-1}]	Fe_d [g kg^{-1}]	pH ($CaCl_2$)	Soil Texture (WRB)	Basal respiration [µg CO_2 h^{-1} g^{-1} dw]
Dikopshof, Universität Bonn, Germany	Haplic Cambisol	1.10	0.14	7.90	7.60	2.55	10.95	6.00	SiL	0.62
Thyrow, Humboldt-Universität Berlin, Germany	Haplic Retisol	0.69	0.08	8.70	6.10	0.39	2.27	5.20	LS	0.49

the pH values of all soil-mineral-monomer mixtures were determined in 0.01 M $CaCl_2$ (soil:solution ratio of 1:5). Because high activities in $^{14}CO_2$ samples at the experimental endpoint of 21 days showed continuous mineralization of goethite-bound citric acid in both soils, the incubation of this treatment was prolonged up to 84 days. CFE was performed after 21 and 84 days yielding identical results for CUE. Glucose solutions were added afterwards, and mineralization measured as described above.

2.6. Phosphate-amended glucose-goethite experiment and oxalate-extractable ^{14}C fraction

Iron-hydroxides are known to strongly bind large quantities of phosphate-P. To test the impact of potential microbial P limitation in goethite-amended incubation experiments, glucose-adsorbed goethite was loaded with phosphate-P and subsequently used for an analogous incubation study. Therefore, 40 mg of freeze-dried, glucose-loaded goethite was resuspended in 1 mL of sterile-filtered 0.1 M NaH_2PO_4 adjusted to pH 5.5. The suspension was shaken for 60 min, centrifuged, the supernatant decanted, and the minerals lyophilized. Following the determination of phosphate-P and ^{14}C in the supernatant, the phosphate-saturated, glucose-loaded goethite was added to the pre-incubated Dikopshof soil in the same goethite topsoil ratio as in the main incubation experiment. The amended soil was incubated for three weeks, and $^{14}CO_2$, microbial biomass, $WEO^{14}C$, and soil ^{14}C were measured in triplicate as described above. Extraction residues from CFE of fumigated and non-fumigated samples were sequentially extracted using acidic oxalate for 4 h in the dark (Schwertmann, 1964), their activity measured afterwards in the extracts.

2.7. Data analysis

Sorption isotherms, cumulative $^{14}CO_2$ evolved over time and mass balances after three weeks of incubation were plotted using Origin Pro 2023b (OriginLab Corporation, Northhampton, Massachusetts, USA). Sorption data was fitted using the Freundlich isotherm (eq. (1)) (Freundlich, 1907):

$$q = K_F C^N \quad \text{(eq. 1)}$$

where q is the number of monomer molecules sorbed (nmol m^{-2} SSA), C is the equilibrium concentration (µmol L^{-1}) and the Freundlich affinity coefficient K_F (describing monomer affinity to mineral surface in nmol m^{-2}/(µmol $ml^{-1})^{1/N}$), as well as N (curvature of the sorption isotherm) as the Freundlich exponent/linearity index. The two-step-desorption experimental data were used to quantify desorbability of OC separately for each desorption step.

The cumulative $^{14}CO_2$ evolution during the initial incubation over three weeks was fitted using a double pseudo-first-order kinetic (eq. (2)):

$$^{14}C\ mineralized\ (\%) = qe1 \times \left(1 - e^{-k1 \times t}\right) + qe2 \times \left(1 - e^{-k2 \times t}\right) \quad \text{(eq. 2)}$$

with the sum of *qe1* and *qe2* describing the fraction of added ^{14}C added being mineralized at t = ∞, *k1* and *k2* as the kinetic rate constants of mineralization and *t* as the time evolved since the start of the incubation in days. Mineralization after glucose priming was corrected for by the amount of soil removed after three weeks for chloroform-fumigation-extraction and $^{14}CO_2$ evolved was fitted using the double pseudo-first order kinetic, with qe3 and qe4 describing ^{14}C mineralized at $t = \infty$ (eq. (3)), as well as *k3* and *k4* as the kinetic rate constants. If the fitted function showed *k3* values above 100 (indicating direct mineralization of the respective fraction), a new model was calculated without kinetic rate constant *k3* (also eq. (3)):

$$^{14}C\ mineralized\ after\ priming\ (\%) = qe3 \times \left(1 - e^{-k3 \times t}\right) + qe4 \times \left(1 - e^{-k4 \times t}\right) \quad \text{(eq.3)}$$

The additional fraction of ^{14}C mineralized after glucose priming was quantified as the difference between the fitted regression models of incubation and priming at t = ∞ (eq. (4)):

$$Priming\ effect\ (\%) = qe3 + qe4 - qe1 - qe2 \quad \text{(eq. 4)}$$

Correlations between sorption and incubation data were analyzed using R Statistical Software (version 4.2, R Core Team, 2022). Boxplots and regression plots were plotted using the ggplot2 package (Wickham, 2016). Histograms and Q-Q plots were used to check data to be normally distributed. Pairwise comparisons were performed using the Wilcoxon-Mann-Whitney-Test (Mann and Whitney, 1947; Wilcoxon, 1945). False discovery rates of pairwise comparisons were controlled using the Bonferroni-Holm method (Holm, 1979).

3. Results

3.1. Sorption and desorption

Non-linear Freundlich isotherms describe the sorption of carboxylic acids to all minerals. In comparison, linear isotherms describe the sorption behavior of phenylalanine and acetylglucosamine (Fig. 1, Supplementary material S4). In general, the quantity of monomers adsorbed per SSA decreased in the following order: goethite > kaolinite > illite (Fig. 1). After desorption in 0.01 M NaN_3 at the second lowest monomer concentration (c = 0.05 µmol ml^{-1}), retained ^{14}C exhibited the same pattern (goethite > kaolinite > illite). The exception was acetylglucosamine, which decreased in the order goethite > illite > kaolinite (Table 2).

3.2. Mineralization

The initial mineralization observed in the first 20-min after homogenization of preincubated soil with monomer-loaded minerals exhibited comparable patterns for both soils without discernible trends for specific minerals or monomers (Fig. 2, Supplementary material S5). The highest initial mineralization (20% of monomer ^{14}C added) was observed for acetylglucosamine adsorbed to goethite in both soils. In contrast, only 0.5–5.1% of ^{14}C was mineralized within acetylglucosamine-clay mineral mesocosms.

Throughout the three weeks of incubation, mineralization fitted well to double pseudo first order kinetics ($R^2 > 0.9$, Supplementary material S6). The highest rates and cumulative mineralization (Fig. 2) were found for citric acid adsorbed to kaolinite and illite in both soils.

In comparison, citric acid adsorbed on goethite in the Thyrow soil showed the lowest fraction of ^{14}C mineralization (22%). The same treatment for the Dikopshof soil yielded a higher mineralized fraction

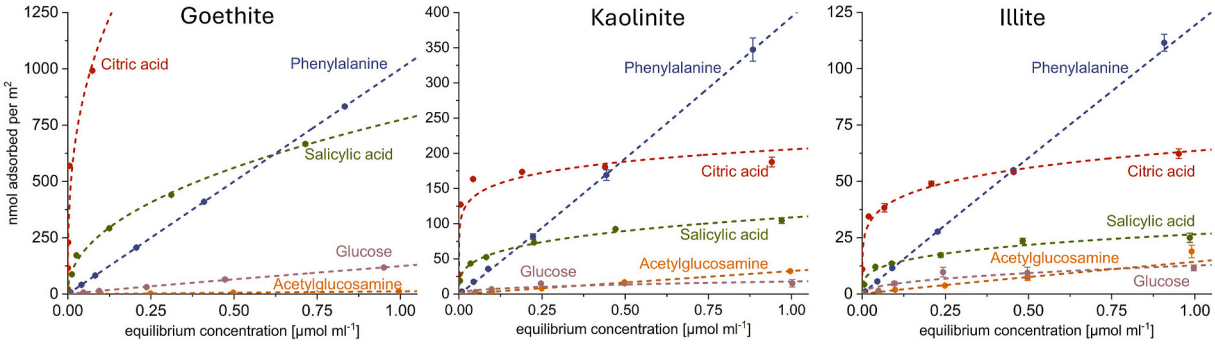

Fig. 1. Freundlich isotherms of adsorption of monomers to goethite (left), kaolinite (middle) and illite (right).

Table 2
Adsorbed monomers [nmol m^{-2}] after 18 h at monomer additions at 0.05 µmol ml^{-1} and 0.5 µmol ml^{-1}. Additionally, the percentage of monomers retained after desorption for 1 h in 0.01 M NaN_3, as well as after the sequential desorption with 0.1 M phosphate are given.

Monomer	concentration added [µM ml^{-1}]	Initially sorbed [nmol m^{-2}]			% retained after desorption using 0.01 M NaN_3			% retained after desorption using 0.1 M PO_4^{3-}		
		Goethite	Kaolinite	Illite	Goethite	Kaolinite	Illite	Goethite	Kaolinite	Illite
Glucose	0.05	7.2 ± 0.2	2.8 ± 0.1	1.4 ± 0.0	94.1 ± 2.3	73.4 ± 6.9	58.1 ± 8.2	54.1 ± 1.2	n.d.	4.2 ± 0.6
	0.5	64.8 ± 5.7	15.3 ± 2.2	8.5 ± 1.3	94.3 ± 6.1	68.3 ± 0.8	77.1 ± 15.2	55 ± 7.3	6.6 ± 3.2	n.d.
Acetylglucosamine	0.05	0.6 ± 0.0	1.7 ± 0.1	0.8 ± 0.1	82.3 ± 4.9	45 ± 6.3	59.2 ± 4.1	11.3 ± 1.1	8 ± 5.7	n.d.
	0.5	6.3 ± 0.7	16.7 ± 0.8	7.1 ± 1.1	71.3 ± 9.2	39.8 ± 12.3	51.3 ± 4.2	n.d.	n.d.	n.d.
Phenylalanine	0.05	20.6 ± 0.8	17.4 ± 0.4	5.6 ± 0.2	92.6 ± 4.4	87.7 ± 0.2	87.4 ± 1.5	16.5 ± 2.3	3.2 ± 1.6	4.4 ± 1.3
	0.5	211.3 ± 4.6	169.1 ± 7.5	54.9 ± 0.6	89.9 ± 1.5	90.7 ± 4.7	87 ± 0.4	16 ± 0.5	4.4 ± 1.3	3.6 ± 1.1
Salicylic acid	0.05	87.7 ± 0.1	43.4 ± 0.2	12.1 ± 0.1	88.6 ± 0.2	80.7 ± 1.2	70.1 ± 1.9	24 ± 0.3	42.2 ± 0.7	54.5 ± 3.6
	0.5	440.5 ± 0.5	92.4 ± 0.7	23.6 ± 1.2	72.2 ± 1.1	79.6 ± 1.7	77.8 ± 13.1	25.8 ± 1.8	34.3 ± 1.5	38.9 ± 5.9
Citric acid	0.05	115 ± 0.0	127.2 ± 0.5	34.4 ± 0.1	99.9 ± 0.0	96.8 ± 0.2	89.7 ± 0.7	29.1 ± 1.4	2.2 ± 0.2	20.7 ± 4.2
	0.5	1134.4 ± 10.5	180.5 ± 0.8	54.1 ± 0.6	93.5 ± 0.4	98.4 ± 0.5	79 ± 1.9	10.6 ± 1.3	10.2 ± 0.8	17.1 ± 3.2

indicating the relevance of the soil for mineralization (59%). In general, the mineralization of substrate bound to goethite was smaller than the one observed for clay mineral-bound substrate. Exceptions were acetylglucosamine, which exhibited high initial mineralization. The same common findings held true for ^{14}C previously bound to goethite assimilated into biomass for both soils (Fig. 3a, Supplementary material S5), except for phenylalanine in Dikopshof soil where biomass-^{14}C was higher for goethite than for illite (Fig. 2).

3.3. Assimilation and carbon use efficiency

Sugars were assimilated to a higher degree in Thyrow soil compared to Dikopshof soil, which contrasted with the results for carboxylic- and amino acid-amended soil. The extremes were exceedingly low amounts of assimilated goethite-sorbed glucose in Dikopshof soil and substantial amounts of assimilated kaolinite-bound acetylglucosamine in Thyrow soil. In fact, up to 100% of the monomer ^{14}C was microbially metabolized in kaolinite-acetylglucosamine incubation experiments with Thyrow soil, while only 52% from the same monomer-mineral combination was microbially processed in Dikopshof soil (Fig. 2).

No such pronounced differences between soils were observed for carboxylic and amino acid-loaded minerals. The assimilation of citric acid into microbial biomass was generally small (Figs. 2 and 3a). Phenylalanine and salicylic acid, on the other hand, demonstrated only slightly different amounts of assimilation in microbial biomass in both soils.

From a mineral perspective, the percentage of ^{14}C retained within the microbial biomass was greater for clay minerals than goethite regardless of soil (Fig. 3a). This difference was greatest for glucose and acetylglucosamine, while carboxylic acids were only marginally assimilated when adsorbed to any mineral. In contrast, ^{14}C retained in soil which was not accounted for by microbial biomass or WEOC was significantly higher for goethite than clay minerals. Similar percentages of organic acids and sugars were retained by goethite (Fig. 3b). Combining retention by assimilation into biomass and sorption to the soil matrix, clays and oxides showed comparable proportions of added ^{14}C retained (Fig. 3c). In absolute terms, however, goethite retained much more carboxylic acid ^{14}C than either kaolinite or illite (Fig. 4).

The CUEs of mineral-adsorbed monomers exhibited a trend like that of assimilation. Goethite exhibited lower CUE values compared to clay minerals: 0.5–23.0% for goethite vs. 0.9–66.4% for illite and kaolinite (Fig. 5, Supplementary material S7). Among sugars, glucose bound to goethite in Dikopshof soil had the lowest CUE of 6.5%. Soil again mattered: monomers in Thyrow soil were processes with a higher CUE

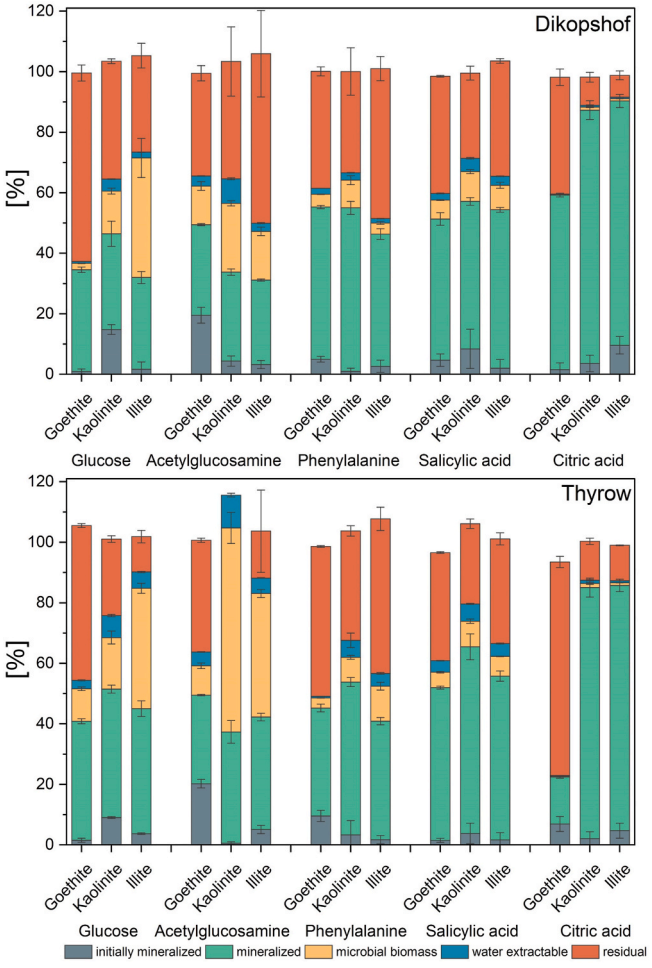

Fig. 2. Fate of monomer-C added adsorbed to goethite, kaolinite or illite incubated in Dikopshof (top) or Thyrow (bottom) soil with different monomers after three weeks of incubation in percent of ^{14}C added, with error bars (n = 3).

values than those in Dikopshof (Fig. 5, Supplementary material S7).

3.4. *Phosphorus deficiencies and mineral retention of fumigated microbial residues*

After three weeks of incubation, goethite-amended soils showed significantly lower PO_4–P concentrations than soils admixed with clay minerals for both soils likely due to P sorption to the added goethite (Fig. 6). Overall, sandy Thyrow soil extracts yielded on average 4 to 5 times higher phosphate-P concentrations than Dikopshof soil extracts because of smaller contents of P-sorbing (hydr)oxides (Table 1).

Microbial processing of goethite-adsorbed glucose in Dikopshof soil increased when goethite was loaded with phosphate prior admixture with soil. The effect was such that mineralization and assimilation of goethite-adsorbed glucose into biomass reached the same levels as that of glucose bound to P-free goethite in Thyrow soil (Table 3).

In principle, microbial OC might have been sorbed to minerals after cellular dissolution with chloroform gas preventing extraction with KCl. To check for retention of microbial OC after the KCl extraction, chloroform fumigated and non-fumigated soil with goethite-bound glucose were sequentially extracted with 2 M KCl and acidic oxalate at pH 3 for 4 h in the dark (Schwertmann, 1964). Sequential extractions yielded comparable results for fumigated and non-fumigated soil (Supplementary material S8). Consequently, retention of microbial assimilated ^{14}C on goethite surfaces after fumigation and extraction with KCl was excluded.

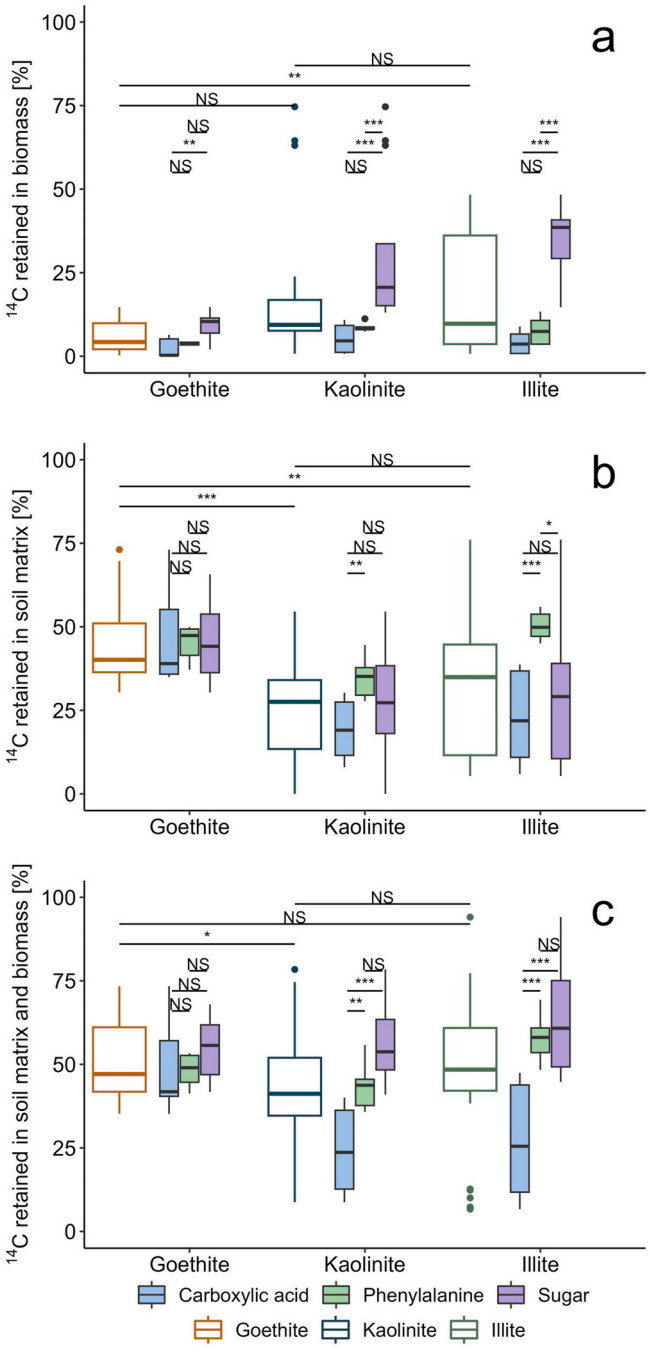

Fig. 3. Fate of goethite-, kaolinite- and illite-adsorbed monomers after three weeks of incubation in Dikopshof and Thyrow soil based on the percentage adsorbed at the start of the experiment, assimilated into microbial biomass (a), retained sorbed onto mineral surfaces or within the soil matrix, i.e. residual fraction (b), and retained within the soil either by assimilation into biomass or by retention within the soil matrix (c). Monomers were grouped into sugars (glucose, acetylglucosamine; n = 12 per mineral), phenylalanine (n = 6 per mineral) and carboxylic acids (salicylic acid, citric acid; n = 12 per mineral). Bonferroni-Holme adjusted pairwise comparisons using Wilcoxon Mann-Whitney tests display significant differences in [%] of monomers retained in biomass, soil matrix or within biomass and soil matrix between goethite and clay mineral amended soil, and differences between sugar (glucose, acetylglucosamine), phenylalanine and carboxylic acids (salicylic acid, citric acid) adsorbed to each mineral. Significance levels: *p ≤ 0.05, **p ≤ 0.01, ***p ≤ 0.001; and NS not significant (p > 0.05).

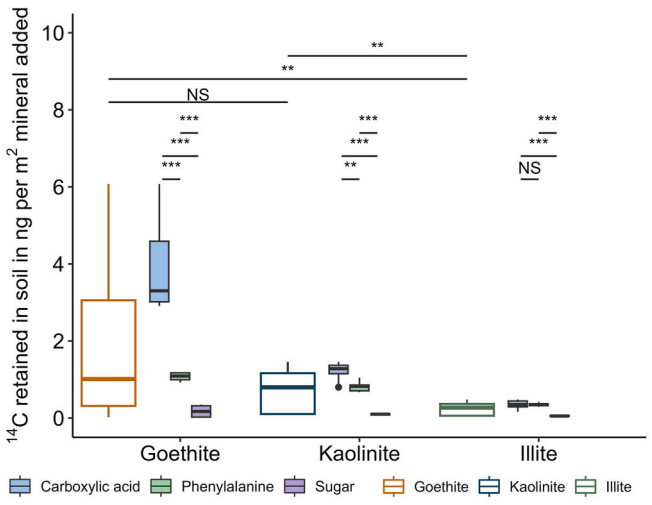

Fig. 4. Nanogram ^{14}C retained per m^2 specific mineral surface area after three weeks of incubation by assimilation into microbial biomass or within soil matrix. Bonferroni-Holme adjusted pairwise comparisons using Wilcoxon Mann-Whitney tests display significant differences in ng C m^{-2} mineral retained between goethite and clay mineral amended soil, and differences between sugar (glucose, acetylglucosamine), phenylalanine and carboxylic acids (salicylic acid, citric acid) adsorbed to each mineral. Significance levels: **p ≤ 0.01, ***p ≤ 0.001; and NS not significant (p > 0.05).

3.5. Linking sorption-desorption behavior and microbial processing

No unified relationship was found between sorption coefficients K_F and microbial processing of sorbed OC (Supplementary material S9). Monomers mattered: High sorption coefficients of organic acids resulted in similar CUEs and ^{14}C assimilation in both soils, while lower K_F values of sugars led to divergent assimilation and CUEs between soils (Supplementary material S9).

No relationship was found also between desorbability and mineralization of monomers in both soils (Fig. 7a). However, the fraction of mineral-associated organic compounds that could be desorbed with 0.01 M NaN_3 after sorption was linearly related with the fraction of microbially assimilated ^{14}C and the CUE for both soils (Fig. 7b–d). The same was observed for total microbial processing of ^{14}C (mineralized + assimilated ^{14}C) in Thyrow soil, but not for Dikopshof soil (Fig. 7c).

3.6. Glucose-induced mineralization

The addition of glucose to mineral-amended soils after three weeks of incubation increased the percentage of mineral-associated monomer ^{14}C that could be mineralized in almost all mesocosms; the exception was illite-bound phenylalanine in Dikopshof soil. The additional ^{14}C mineralization was significantly larger for goethite treatments compared to kaolinite (Fig. 8a). Only for Thyrow soil, additional $^{14}CO_2$ released due to glucose additions increased with increasing ^{14}C retained in the soil matrix after the first three weeks of incubation primarily in goethite-amended soils (Fig. 8b and c). No changes of soil pH were observed during the incubation experiment (Dikopshof: pH 6.04 ± 0.03, Thyrow: pH 5.04 ± 0.02).

4. Discussion

4.1. Sorptive control of microbial processing of mineral associated monomers

The superior ability of goethite, and Fe-(hydr)oxides in general, over clay minerals to sorb and retain dissolved OC, and preserve mineral-associated organic carbon (MAOC) has been demonstrated in both laboratory (Saidy et al., 2013; Yeasmin et al., 2014) and field studies (Bramble et al., 2024). Our batch sorption study yielded similar results (Fig. 1), with goethite sorbing more of all monomers than kaolinite and illite on a per surface area basis, with the exception of acetylglucosamine. These findings align with Yeasmin et al. (2014), who observed similar sorption capacity for glucose on goethite under batch conditions with ^{14}C-labeled monomers in 0.01 M NaN_3, though at an equilibrium pH rather than at a fixed pH 5.5. However, retention of OC after desorption in our study differed slightly; Yeasmin et al. (2014) observed higher retention of citric acid on goethite and kaolinite and greater binding of citric acid and phenylalanine on illite.

Sorption strength and desorbability alone explained neither initial mineralization in the first 20 min nor total mineralization after three weeks. For instance, more than 40% of total mineralization of goethite-bound acetylglucosamine occurred in the first 20 min. These levels are in line with mineralization rates of up to 1.1% per minute for glucose added to soil found in the literature (Gunina and Kuzyakov, 2015). Rinsing ^{14}C-loaded minerals with water after sorption could have reduced the introduction of non-adsorbed and thus easily mineralizable OC into soil. Instead, we only decanted supernatants, and minerals were not rinsed to avoid desorption. For monomers with marginal sorption to

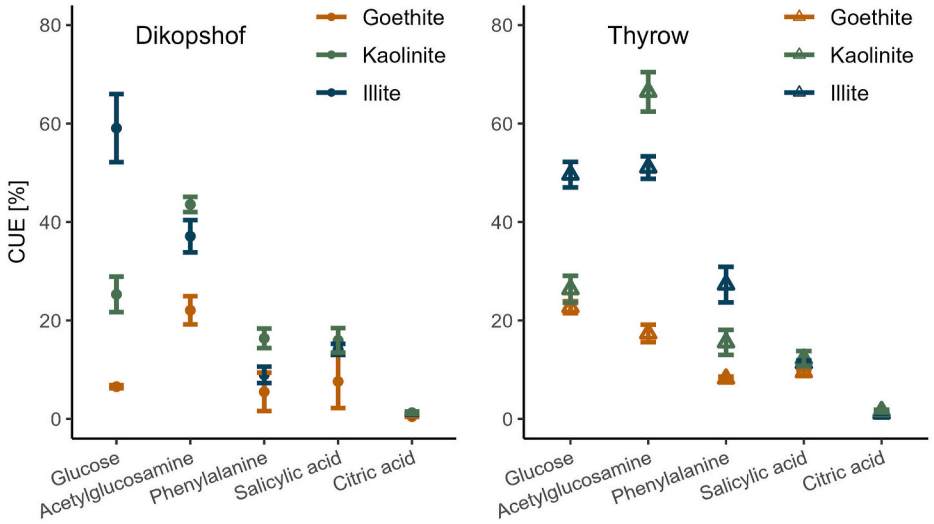

Fig. 5. Microbial carbon use efficiencies of monomers adsorbed to minerals incubated in either Dikopshof (left), or Thyrow (right) soil after three weeks of incubation.

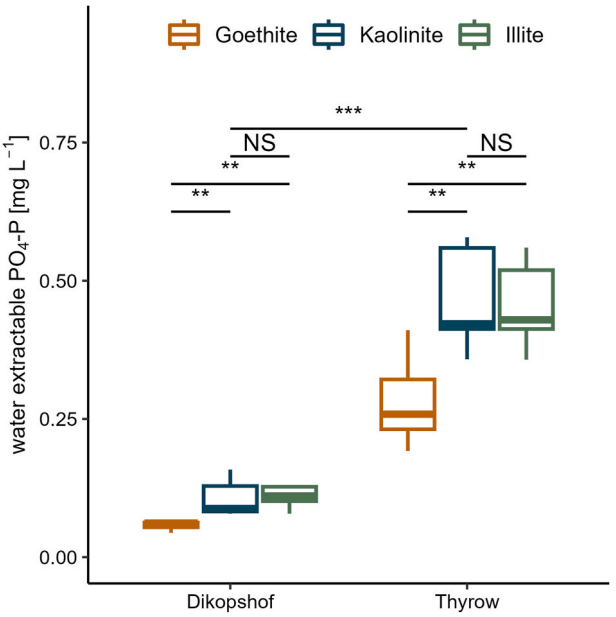

Fig. 6. Phosphate concentrations after three weeks of incubation in 2 M KCl soil extracts (w/v ratio 1:5) grouped by minerals and soil. Bonferroni-Holme adjusted pairwise comparisons using Wilcoxon Mann-Whitney tests display significant differences in phosphate concentrations between goethite and clay mineral amended soil, and overall differences between Dikopshof and Thyrow soil. Significance levels: **p ≤ 0.01, ***p ≤ 0.001; and NS not significant (p > 0.05). One incubated sample per mineral x monomer x soil treatment was analyzed, thus each box consists of 21 replicates.

minerals—glucose and acetylglucosamine (Fig. 1)—a majority of ^{14}C remained within the supernatant, which would increase the potential for error during decantation. This could explain the high initial mineralization observed in some mesocosms, like glucose bound to kaolinite or acetylglucosamine bound to goethite.

Conversely, this would not apply to goethite-adsorbed citric acid and (to some extent) salicylic acid as high mineralization was observed despite <0.1% of added OC being recovered from the supernatant. Rapid initial mineralization of monomers with higher sorption coefficients may be driven by OC sorbed to more accessible binding sites such as external surfaces with shorter diffusion distances to microorganisms, which is likely due to adsorption of monomers below observable saturation points. Edge-bound monomers could also have been more easily removed by exchange with dissolved organic matter and nutrients in the soil solution. This effect might be stronger for monomers bound via ligand-exchange reactions (e.g., monomers containing carboxyl-groups) as shown by phosphate-induced desorption (Table 2). Comparatively more phosphate in Thyrow soil extracts than in those of Dikopshof soil (Fig. 6) thus would be a reason for rapid mineralization of goethite-bound citric acid observed in the former. Furthermore, hydrophobic OC can displace sorbed hydrophilic OC—i.e., all monomers in the experiment—from mineral phases (Kaiser and Zech, 1997). Competitive sorption therefore can be a plausible cause for rapid mineralization for all monomers used in this study, not just organic acids. Subsequent microbial processing would have been fueled by OC adsorbed within mineral pores and is therefore rate-limited by diffusion of new sorbates as well as desorption of monomers (Pignatello and Xing, 1996).

Results for citric acid adsorbed to goethite suggest that ligand exchange can be effective at reducing mineralization and overall microbial processing. Most of the citric acid sorbed to goethite at pH 5.5 was mineralized in Dikopshof soil (pH > 5.5), while only 29% was mineralized in Thyrow soil (pH < 5.5). Introduction into Dikopshof soil brought goethite closer to its point of zero charge (PZC). As the pH approaches the PZC, goethite surfaces became less positively charged (Filius et al., 2000), reducing electrostatic attraction between (partly, pH < pKa3) deprotonated citric acid and mineral surface, potentially causing additional monomers to desorb. Adding goethite to Thyrow soil on the other hand brought the mineral further away from its PZC, increasing electrostatic attraction of the sorbate. This might also explain the relationship found in Thyrow, but not Dikopshof soil for desorbability determined at pH 5.5 and the overall amount of microbially processed monomer-C (Fig. 7c). Interestingly, differences between the magnitudes of microbial processing of goethite-adsorbed monomers incubated in both soils decreased with increasing desorbability for carboxyl-group–containing monomers as well as glucose and acetylglucosamine. In fact, pH-dependent differences in the amount of microbially processed monomers between soils found for organic acids is reversed for glucose (Thyrow > Dikopshof) as more OC would be adsorbed through hydrogen bonding at higher pH (Olsson et al., 2011). Clay minerals, in contrast, were characterized by overall higher desorbability and microbial processing when compared to goethite. However, microbial processing increased together with desorbability only in sandy Thyrow soil. In clay-rich, aggregated Dikopshof soil, high desorbability might have been counteracted by re-adsorption of desorbed monomers onto native clay minerals or pedogenic oxides, or diffusion into aggregates away from decomposer (Lehmann and Kleber, 2015).

4.2. *Biological processing of mineral-associated monomers*

Our results indicate that OC assimilated into biomass relative to microbially processed OC — that is CUE — is linearly related to the fraction of mineral adsorbed monomers extractable with 0.01 M NaN_3 and thus the reversibility of sorption (Fig. 7d), instead of sorption strength. Two control levels of CUE are at work as Schimel (2023) has pointed out. First, biochemical pathways and substrate chemistry limit the percentage of substrate-C that can be assimilated. Second, environmental and physiological conditions force the microbiome to regulate its biochemistry to optimize fitness. The first is exhibited by the low biochemically possible CUE of carboxylic acids, which are not easily desorbed from iron oxides and clay minerals (Jones and Edwards, 1998; Yeasmin et al., 2014) but are also readily metabolized for gaining energy. Citric acid, for example, is central to energy-yielding metabolism and specifically the tricarboxylic acid cycle. Hence, the low CUE of carboxylic acids was rather related to their biochemical processing than to their low desorbability. In line with the low CUE in our incubation experiment, the CUE of citric acid in a topsoil from an Eutric Cambisol grassland was 24 ± 4 % (Brown and Jones, 2024). This also applies to salicylic acid which has an average CUE in arable soils below 20% (Jones et al., 2018).

Table 3
Fate of uniformly ^{14}C labeled glucose adsorbed to either goethite or phosphate-loaded goethite after three weeks of incubation in either Dikopshof or Thyrow soil.

Soil	Mineral	initial mineralization [%]	mineralized [%]	biomass [%]	WEOC [%]	residual [%]	microbially processed [%]	CUE [%]	mass balance [%]
Dikopshof	Goethite	1.0 ± 0.8	30.5 ± 0.5	2.1 ± 0.1	0.6 ± 0.0	62.3 ± 2.7	32.7 ± 0.5	6.5 ± 0.3	95.5 ± 2.2
Dikopshof	PO_4^{3-} loaded goethite	0.0 ± 0.0	35.6 ± 0.0	11.1 ± 0.1	1.7 ± 0.0	50 ± 1.6	46.6 ± 0.1	23.7 ± 0.2	98.3 ± 1.8
Thyrow	Goethite	1.6 ± 0.7	36.6 ± 0.7	10.8 ± 0.6	2.8 ± 0.1	51.1 ± 0.7	47.4 ± 0.5	22.7 ± 1.2	101.3 ± 0.7

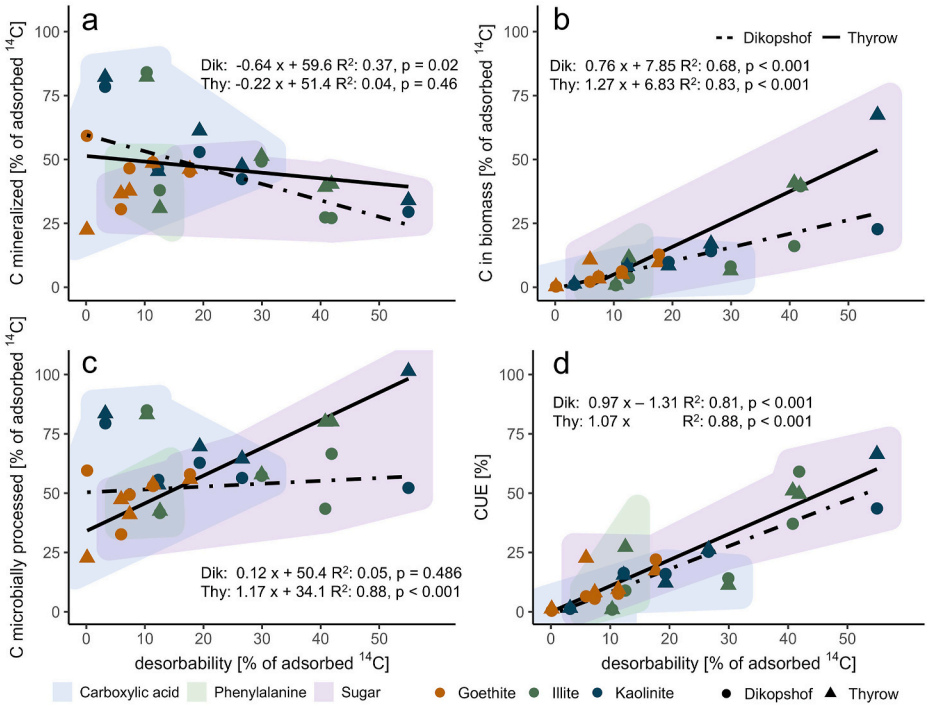

Fig. 7. Correlation between the mean values for ^{14}C desorbed from minerals after shaking with 0.01 M NaN_3 in batch sorption studies (mean STD: 2.87 %, Table 2) and mineral-adsorbed ^{14}C mineralized after three weeks of incubation (a), assimilated into biomass (b), microbially metabolized (c) and microbial carbon use efficiency (d) in Dikopshof (Dik) and Thyrow (Thy) soil (mean STD: 1.99 %, Supplementary Information S7). Monomers were grouped as carboxylic acids (salicylic acid, citric acid), phenylalanine (as the only amino acid) and sugars (glucose, acetylglucosamine).

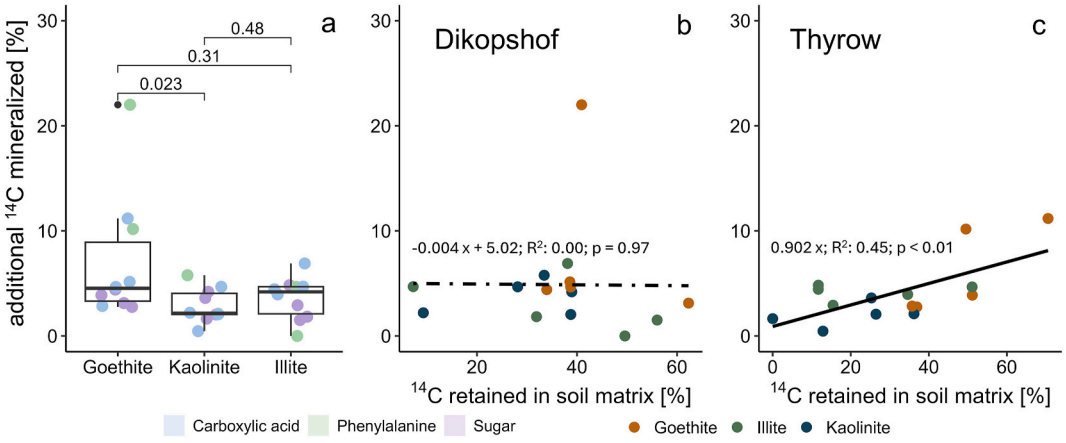

Fig. 8. Effect of glucose-induced priming on the mineralization of mineral adsorbed monomer ^{14}C. Monomer ^{14}C adsorbed to goethite was mineralized to a significantly larger extend than ^{14}C adsorbed to kaolinite after priming (a). While no correlation was found between the percentage of monomer-C retained in soils after three weeks of incubation and the additional mineralization after glucose addition in Dikopshof soil (b), the fraction of $^{14}CO_2$ released due to priming increased with the fraction of ^{14}C retained in the soil matrix for the Thyrow soil (c).

However, the CUE of goethite-adsorbed glucose in Dikopshof soil was as low as 7%, despite typical CUEs of glucose in soil around 40% (Schimel, 2023) and highest values around 75% (Sugai and Schimel, 1993). In general, CUE for goethite-sorbed monomers were lower than those for monomers adsorbed to clay minerals. These findings suggest that environmental and physiological conditions restricted the microbial processing of monomers sorbed to goethite. Goethite efficiently binds phosphate (Antelo et al., 2005; Geelhoed et al., 1998) and organic P (Amadou et al., 2022). Therefore, microbial communities in goethite-amended mesocosms might have encountered P limitations (Fig. 6). Such P limitation was confirmed for the Dikopshof soil since CUE, assimilation and mineralization of goethite-bound glucose increased to levels comparable to Thyrow soil after loading goethite with P (Table 3). Minerals incorporated into soil therefore remain micro-habitats of microbial activity responding to altered nutrient availability. Similar findings were observed in a field study with mineral bags buried in topsoil of grasslands in southern Germany (Brandt et al., 2023). In that study, retrieved goethite with adsorbed organic matter had lower phospholipid fatty acid (PLFA) to OC ratios and higher enzyme activities in C-, N-, and P-cycling than illite, thus suggesting goethite induced C, N and P deficiencies while illite-bound OM and nutrients desorbed more readily and were more accessible for the microbiome (Brandt et al., 2023).

In our study, sugars bound to clay minerals desorbed more easily and

were assimilated to a greater extent. The efficient assimilation of sugars into microbial biomass is promoted by their biochemical processing. Hence, the linear relationship between desorbability and CUE was also caused by the combination of efficient biochemical assimilation and desorption of sugars.

CUE also depends on cellular maintenance and thus can be modified by stress (Schimel, 2023). The physical effect of clay minerals and iron (hydr-)oxides on resident microorganisms can induce cellular stress, with greater stress typically in the latter than the former. For instance, the needle-like structures of goethite have been demonstrated to penetrate the peptidoglycan layers of bacteria and outer cell membrane (Glasauer et al., 2001). A strain of *Escherichia coli* also showed reduced growth and protective biofilm formation when in contact with goethite while contact with kaolinite and montmorillonite, in contrast, promoted growth (Cai et al., 2018). Thus, in our study, clay mineral-influenced microhabitats would have been conducive to microbial growth whereas goethite would have been hostile.

Our results also show that additional MAOC can be mineralized after glucose application (Fig. 8, Supplementary material S5, S6). Priming is the most likely explanation: Glucose provides an energy-rich substrate that can increase exo-enzyme production and more mineralization of MAOC. Our findings of additional MAOC mineralization after glucose addition are consistent with other studies (Jilling et al., 2021; Li et al., 2021). Specifically, in Thyrow soil (Fig. 8c), goethite-adsorbed organic acids were strongly retained in incubations without glucose, but became available for microbial processing to a larger extent after glucose application. In Dikopshof, by comparison, a lack of glucose-enhanced mineralization was most likely due to desorption of ligand-bound monomers caused by the soil's pH before glucose was added. This desorption caused an effective mineralization of goethite sorbed monomers so that only very little of them was available for priming-induced mineralization after the first three-week incubation. Either way, organic acids retained by the soil mineral phase may be more prone to release and mineralization upon glucose-induced priming. However, the extent of additional MAOC mineralization after glucose addition was small compared to the fraction of monomer C originally retained.

4.3. Implications for C cycling in soil

It is prudent to consider the experimental context when applying our results to arable soils in field settings. Our study traced the fate of mineral-associated monomers for only three weeks, during which monomers adsorbed to clay minerals were assimilated more efficiently into microbial biomass than those on goethite (Figs. 3a and 5). However, the long-term retention of ensuing microbial necromass, potentially through spatial exclusion (Balesdent et al., 2000; Rasmussen et al., 2005) or re-adsorption to minerals (Angst et al., 2018; Cotrufo et al., 2013), cannot be assessed within this timeframe. Nonetheless, microbial necromass could significantly contribute to soil OC formation, especially in arable soils, depending on microbial death pathways (Camenzind et al., 2023). Additionally, this study isolated individual minerals, while in natural soils, clay minerals and pedogenic iron oxides often co-occur. Field observations (Bramble et al., 2024; Brandt et al., 2023) support similar differences between iron (hydr-)oxides and illite, albeit also with isolated minerals. Our observation that goethite sorbs and retains organic compounds more efficiently than illite (Figs. 3c and 4) may vary in soils where these minerals are intermixed. However, studies in arable soils of the humid tropics, with varying contents of kaolinite, gibbsite, and goethite, reveal that soils with a high oxide-to-clay mineral ratio exhibit reduced microbial respiration and greater retention of MAOC over extended incubation (Kirsten et al., 2021). Thus, the observed behavior of carboxylic acids likely highlights key differences between oxides and clay minerals and underscores their distinct roles in C cycling within soil systems.

5. Conclusions

Assimilation of organic monomers associated with minerals into microbial biomass and the resulting CUE increase linearly with desorbability. Monomers initially adsorbed to clay minerals were retained in the soil primarily through stabilization within the microbial biomass. In contrast, a majority of monomer-C adsorbed to goethite remained sorbed to the soil matrix. However, part of this C can be desorbed and microbially cycled with comparatively low CUE. Our results highlighted the quantitative importance of small organic acid sorption to soils for overall C sequestration, substantiating the relevance of future research of this process. Although the findings of our laboratory experiments are in line with field observations, factors like nutrient availability at mineral surfaces, fluctuating temperatures and wet-dry cycles may influence the retention of mineral-associated organic matter in the environment.

CRediT authorship contribution statement

Alexander Konrad: Writing – review & editing, Writing – original draft, Visualization, Software, Methodology, Investigation, Formal analysis, Data curation, Conceptualization. **Diana Hofmann:** Writing – review & editing, Visualization, Validation, Supervision, Methodology, Investigation. **Jan Siemens:** Writing – review & editing, Validation, Supervision, Project administration, Funding acquisition, Data curation, Conceptualization. **Kenton P. Stutz:** Writing – review & editing, Visualization, Validation, Supervision, Resources, Project administration, Investigation, Funding acquisition, Conceptualization. **Friederike Lang:** Writing – review & editing, Supervision, Project administration, Investigation, Funding acquisition, Conceptualization. **Ines Mulder:** Writing – review & editing, Writing – original draft, Visualization, Validation, Supervision, Project administration, Investigation, Funding acquisition, Data curation, Conceptualization.

Declaration of competing interest

The authors declare that they have no known competing financial interests of personal relationships that could have appeared to influence the work reported in this paper.

Acknowledgements

This work was funded by the German Research Foundation (DFG, grant no. 465123895). Experimental data were obtained within the DFG Priority Program 2322 "SoilSystems". We thank the staff of the core projects, the SPP office and the BExIS team for their work in maintaining the project infrastructure, and the SPP Scientific Committee for their role in setting up the SPP project. Soils were provided by S.J. Seidel and H. Hüging (University of Bonn, Germany), and K. Schweitzer and M. Baumecker (Humboldt-Universität zu Berlin, Germany). We would also like to thank Prof. Dr. Elena Evguenieva-Hackenberg and Andreas Jäger for their management of the radioactive control area at the Justus-Liebig-University Giessen. We would like to extend our gratitude to Andrea Ecker, Simon Horn, and Stefan Köppchen for their invaluable assistance in the radioactive control area at Forschungszentrum Jülich when we were running out of time and hands. We thank Klaus Kaiser, University of Halle, for his feedback and inspiring discussions.

Appendix A. Supplementary data

Supplementary data to this article can be found online at https://doi.org/10.1016/j.soilbio.2025.109740.

References

Amadou, I., Faucon, M.-P., Houben, D., 2022. Role of soil minerals on organic phosphorus availability and phosphorus uptake by plants. Geoderma 428, 116125. https://doi.org/10.1016/j.geoderma.2022.116125.

Angst, G., Messinger, J., Greiner, M., Häusler, W., Hertel, D., Kirfel, K., et al., 2018. Soil organic carbon stocks in topsoil and subsoil controlled by parent material, carbon input in the rhizosphere, and microbial-derived compounds. Soil Biology and Biochemistry 122, 19–30. https://doi.org/10.1016/j.soilbio.2018.03.026.

Angst, G., Mueller, K.E., Nierop, K.G.J., Simpson, M.J., 2021. Plant- or microbial-derived? A review on the molecular composition of stabilized soil organic matter. Soil Biology and Biochemistry 156, 108189. https://doi.org/10.1016/j.soilbio.2021.108189.

Antelo, J., Avena, M., Fiol, S., López, R., Arce, F., 2005. Effects of pH and ionic strength on the adsorption of phosphate and arsenate at the goethite–water interface. Journal of Colloid and Interface Science 285 (2), 476–486. https://doi.org/10.1016/j.jcis.2004.12.032.

Balesdent, J., Chenu, C., Balabane, M., 2000. Relationship of soil organic matter dynamics to physical protection and tillage. Soil and Tillage Research 53 (3–4), 215–230. https://doi.org/10.1016/S0167-1987(99)00107-5.

Berendsen, R.L., Pieterse, C.M.J., Bakker, P.A.H.M., 2012. The rhizosphere microbiome and plant health. Trends in Plant Science 17 (8), 478–486. https://doi.org/10.1016/j.tplants.2012.04.001.

Blagodatskaya, E.V., Blagodatsky, S.A., Anderson, T.-H., Kuzyakov, Y., 2009. Contrasting effects of glucose, living roots and maize straw on microbial growth kinetics and substrate availability in soil. European Journal of Soil Science 60 (2), 186–197. https://doi.org/10.1111/j.1365-2389.2008.01103.x.

Boos, E.F., Magid, J., Bruun, S., Jørgensen, N.O.G., 2022. Liquid scintillation counting can underestimate 14C-activity of 14CO2 trapped in NaOH. Soil Biology and Biochemistry 166, 108576. https://doi.org/10.1016/j.soilbio.2022.108576.

Boos, E.F., Bruun, S., Magid, J., 2023. Priming is frequently overestimated in studies using 14C-labelled substrates due to underestimation of 14CO2 activity. Soil Biology and Biochemistry 181, 109020. https://doi.org/10.1016/j.soilbio.2023.109020.

Bramble, D.S.E., Ulrich, S., Schöning, I., Mikutta, R., Brandt, L., Poll, C., et al., 2024. Formation of mineral-associated organic matter in temperate soils is primarily controlled by mineral type and modified by land use and management intensity. Global Change Biology 30 (1), e17024. https://doi.org/10.1111/gcb.17024.

Brandt, L., Stache, F., Poll, C., Bramble, D.S., Schöning, I., Schrumpf, M., et al., 2023. Mineral type and land-use intensity control composition and functions of microorganisms colonizing pristine minerals in grassland soils. Soil Biology and Biochemistry 182, 109037. https://doi.org/10.1016/j.soilbio.2023.109037.

Brown, R.W., Jones, D.L., 2024. Plasticity of microbial substrate carbon use efficiency in response to changes in plant carbon input and soil organic matter status. Soil Biology and Biochemistry 188, 109230. https://doi.org/10.1016/j.soilbio.2023.109230.

Cabrol, L., Quéméneur, M., Misson, B., 2017. Inhibitory effects of sodium azide on microbial growth in experimental resuspension of marine sediment. Journal of Microbiological Methods 133, 62–65. https://doi.org/10.1016/j.mimet.2016.12.021.

Cai, P., Liu, X., Ji, D., Yang, S., Walker, S.L., Wu, Y., et al., 2018. Impact of soil clay minerals on growth, biofilm formation, and virulence gene expression of Escherichia coli O157:H7. Environmental Pollution 243, 953–960. https://doi.org/10.1016/j.envpol.2018.09.032.

Camenzind, T., Mason-Jones, K., Mansour, I., Rillig, M.C., Lehmann, J., 2023. Formation of necromass-derived soil organic carbon determined by microbial death pathways. Nature Geoscience 16 (2), 115–122. https://doi.org/10.1038/s41561-022-01100-3.

Cornell, R.M., Schwertmann, U., 2003. *The iron oxides: structure, properties, reactions, occurrences and uses* (2. Compl. Rev. And Extended ed., Repr). Wiley-VCH, Weinheim.

Cotrufo, M.F., Wallenstein, M.D., Boot, C.M., Denef, K., Paul, E., 2013. The Microbial Efficiency-Matrix Stabilization (MEMS) framework integrates plant litter decomposition with soil organic matter stabilization: do labile plant inputs form stable soil organic matter? Global Change Biology 19 (4), 988–995. https://doi.org/10.1111/gcb.12113.

Dalkmann, P., Willaschek, E., Schiedung, H., Bornemann, L., Siebe, C., Siemens, J., 2014. Long-term wastewater irrigation reduces sulfamethoxazole sorption, but not ciprofloxacin binding, in Mexican soils. Journal of Environmental Quality 43 (3), 964–970. https://doi.org/10.2134/jeq2013.11.0473.

Dultz, S., Woche, S.K., Mikutta, R., Schrapel, M., Guggenberger, G., 2019. Size and charge constraints in microaggregation: Model experiments with mineral particle size fractions. Applied Clay Science 170, 29–40. https://doi.org/10.1016/j.clay.2019.01.002.

Fang, Y., Fu, J., Tao, C., Liu, P., Cui, B., 2020. Mechanical properties and antibacterial activities of novel starch-based composite films incorporated with salicylic acid. International Journal of Biological Macromolecules 155, 1350–1358. https://doi.org/10.1016/j.ijbiomac.2019.11.110.

Feng, W., Plante, A.F., Six, J., 2013. Improving estimates of maximal organic carbon stabilization by fine soil particles. Biogeochemistry 112 (1–3), 81–93. https://doi.org/10.1007/s10533-011-9679-7.

Filius, J.D., Lumsdon, D.G., Meeussen, J.C.L., Hiemstra, T., Van Riemsdijk, W.H., 2000. Adsorption of fulvic acid on goethite. Geochimica et Cosmochimica Acta 64 (1), 51–60. https://doi.org/10.1016/S0016-7037(99)00176-3.

Freundlich, H., 1907. Über die Adsorption in Lösungen. Zeitschrift für Physikalische Chemie 57U (1), 385–470. https://doi.org/10.1515/zpch-1907-5723.

Gao, J., Jansen, B., Cerli, C., Helmus, R., Mikutta, R., Dultz, S., et al., 2018. Organic matter coatings of soil minerals affect adsorptive interactions with phenolic and amino acids. European Journal of Soil Science 69 (4), 613–624. https://doi.org/10.1111/ejss.12562.

Geelhoed, J.S., Hiemstra, T., Van Riemsdijk, W.H., 1998. Competitive interaction between phosphate and citrate on goethite. Environmental Science & Technology 32 (14), 2119–2123. https://doi.org/10.1021/es970908y.

Georgiou, K., Jackson, R.B., Vindušková, O., Abramoff, R.Z., Ahlström, A., Feng, W., et al., 2022. Global stocks and capacity of mineral-associated soil organic carbon. Nature Communications 13 (1), 3797. https://doi.org/10.1038/s41467-022-31540-9.

Glasauer, S., Langley, S., Beveridge, T.J., 2001. Sorption of Fe (Hydr)Oxides to the surface of *Shewanella putrefaciens* : cell-bound fine-grained minerals are not always formed de novo. Applied and Environmental Microbiology 67 (12), 5544–5550. https://doi.org/10.1128/AEM.67.12.5544-5550.2001.

Gunina, A., Kuzyakov, Y., 2015. Sugars in soil and sweets for microorganisms: review of origin, content, composition and fate. Soil Biology and Biochemistry 90, 87–100. https://doi.org/10.1016/j.soilbio.2015.07.021.

Holm, S., 1979. A Simple Sequentially Rejective Multiple Test Procedure. Scand J Statist. https://doi.org/10.2307/4615733.

Hütsch, B.W., Augustin, J., Merbach, W., 2002. Plant rhizodeposition — an important source for carbon turnover in soils. Journal of Plant Nutrition and Soil Science 165 (4), 397–407. https://doi.org/10.1002/1522-2624(200208)165:4<397::AID-JPLN397>3.0.CO;2-C.

Jilling, A., Keiluweit, M., Gutknecht, J.L.M., Grandy, A.S., 2021. Priming mechanisms providing plants and microbes access to mineral-associated organic matter. Soil Biology and Biochemistry 158, 108265. https://doi.org/10.1016/j.soilbio.2021.108265.

Jones, D.L., Edwards, A.C., 1998. Influence of sorption on the biological utilization of two simple carbon substrates. Soil Biology and Biochemistry 30 (14), 1895–1902. https://doi.org/10.1016/S0038-0717(98)00060-1.

Jones, D.L., Hill, P.W., Smith, A.R., Farrell, M., Ge, T., Banning, N.C., Murphy, D.V., 2018. Role of substrate supply on microbial carbon use efficiency and its role in interpreting soil microbial community-level physiological profiles (CLPP). Soil Biology and Biochemistry 123, 1–6. https://doi.org/10.1016/j.soilbio.2018.04.014.

Kaiser, K., Zech, W., 1997. Competitive sorption of dissolved organic matter fractions to soils and related mineral phases. Soil Science Society of America Journal 61 (1), 64–69. https://doi.org/10.2136/sssaj1997.03615995006100010011x.

Kalbitz, K., Schwesig, D., Rethemeyer, J., Matzner, E., 2005. Stabilization of dissolved organic matter by sorption to the mineral soil. Soil Biology and Biochemistry 37 (7), 1319–1331. https://doi.org/10.1016/j.soilbio.2004.11.028.

Kandeler, E., Gebala, A., Boeddinghaus, R.S., Müller, K., Rennert, T., Soares, M., et al., 2019. The mineralosphere – succession and physiology of bacteria and fungi colonising pristine minerals in grassland soils under different land-use intensities. Soil Biology and Biochemistry 136, 107534. https://doi.org/10.1016/j.soilbio.2019.107534.

Khan, N., Bano, A., Curá, J.A., 2020. Role of beneficial microorganisms and salicylic acid in improving rainfed agriculture and future food safety. Microorganisms 8 (7), 1018. https://doi.org/10.3390/microorganisms8071018.

Kirsten, M., Mikutta, R., Vogel, C., Thompson, A., Mueller, C.W., Kimaro, D.N., et al., 2021. Iron oxides and aluminous clays selectively control soil carbon storage and stability in the humid tropics. Scientific Reports 11 (1), 5076. https://doi.org/10.1038/s41598-021-84777-7.

Kleber, M., Mikutta, R., Torn, M.S., Jahn, R., 2005. Poorly crystalline mineral phases protect organic matter in acid subsoil horizons. European Journal of Soil Science 0 (0), 050912034650054. https://doi.org/10.1111/j.1365-2389.2005.00706.x.

Kleber, Markus, Bourg, I.C., Coward, E.K., Hansel, C.M., Myneni, S.C.B., Nunan, N., 2021. Dynamic interactions at the mineral–organic matter interface. Nature Reviews Earth & Environment 2 (6), 402–421. https://doi.org/10.1038/s43017-021-00162-y.

Kuzyakov, Y., Domanski, G., 2000. Carbon input by plants into the soil. Review. Journal of Plant Nutrition and Soil Science 163 (4), 421–431. https://doi.org/10.1002/1522-2624(200008)163:4<421::AID-JPLN421>3.0.CO;2-R.

Lehmann, J., Kleber, M., 2015. The contentious nature of soil organic matter. Nature 528 (7580), 60–68. https://doi.org/10.1038/nature16069.

Lehmann, J., Hansel, C.M., Kaiser, C., Kleber, M., Maher, K., Manzoni, S., et al., 2020. Persistence of soil organic carbon caused by functional complexity. Nature Geoscience 13 (8), 529–534. https://doi.org/10.1038/s41561-020-0612-3.

Li, H., Bölscher, T., Winnick, M., Tfaily, M.M., Cardon, Z.G., Keiluweit, M., 2021. Simple plant and microbial exudates destabilize mineral-associated organic matter via multiple pathways. Environmental Science & Technology 55 (5), 3389–3398. https://doi.org/10.1021/acs.est.0c04592.

Lorenz, M., Blagodatskaya, E., Finn, D., Fricke, C., Hüging, H., Kandeler, E., et al., 2024. Database for the priority program 2322 SoilSystems – soils and substrates used in the first phase (2021-2024). Zenodo. https://doi.org/10.5281/zenodo.11207502 [Data set].

Mann, H.B., Whitney, D.R., 1947. On a test of whether one of two random variables is stochastically larger than the other. The Annals of Mathematical Statistics 18 (1), 50–60. https://doi.org/10.1214/aoms/1177730491.

Mikutta, R., Mikutta, C., Kalbitz, K., Scheel, T., Kaiser, K., Jahn, R., 2007. Biodegradation of forest floor organic matter bound to minerals via different binding mechanisms. Geochimica et Cosmochimica Acta 71 (10), 2569–2590. https://doi.org/10.1016/j.gca.2007.03.002.

Murage, E.W., Voroney, P.R., 2007. Modification of the original chloroform fumigation extraction technique to allow measurement of δ13C of soil microbial biomass carbon. Soil Biology and Biochemistry 39 (7), 1724–1729. https://doi.org/10.1016/j.soilbio.2007.01.026.

OECD, 2000. Test No. 106: Adsorption – Desorption Using a Batch Equilibrium Method. OECD. https://doi.org/10.1787/9789264069602-en.
OECD, 2002. Test No. 307: Aerobic and Anaerobic Transformation in Soil. OECD. https://doi.org/10.1787/9789264070509-en.
Olsson, R., Giesler, R., Persson, P., 2011. Adsorption mechanisms of glucose in aqueous goethite suspensions. Journal of Colloid and Interface Science 353 (1), 263–268. https://doi.org/10.1016/j.jcis.2010.09.023.
Pignatello, J.J., Xing, B., 1996. Mechanisms of slow sorption of organic chemicals to natural particles. Environmental Science & Technology 30 (1), 1–11. https://doi.org/10.1021/es940683g.
R Core Team, 2022. R: A Language and Environment for Statistical Computing (n.d.). R Foundation for Statistical Computing, Vienna, Austra. Retrieved from. https://www.R-project.org/.
Rasmussen, C., Torn, M.S., Southard, R.J., 2005. Mineral assemblage and aggregates control carbon dynamics in a California conifer forest. Soil Science Society of America Journal 69 (6), 1711–1721. https://doi.org/10.2136/sssaj2005.0040.
Saidy, A.R., Smernik, R.J., Baldock, J.A., Kaiser, K., Sanderman, J., 2013. The sorption of organic carbon onto differing clay minerals in the presence and absence of hydrous iron oxide. Geoderma 209–210, 15–21. https://doi.org/10.1016/j.geoderma.2013.05.026.
Saidy, A.R., Smernik, R.J., Baldock, J.A., Kaiser, K., Sanderman, J., 2015. Microbial degradation of organic carbon sorbed to phyllosilicate clays with and without hydrous iron oxide coating: mineralization of OC-clay-oxide associations. European Journal of Soil Science 66 (1), 83–94. https://doi.org/10.1111/ejss.12180.
Schimel, J., 2023. Modeling ecosystem-scale carbon dynamics in soil: the microbial dimension. Soil Biology and Biochemistry 178, 108948. https://doi.org/10.1016/j.soilbio.2023.108948.
Schrumpf, M., Kaiser, K., Guggenberger, G., Persson, T., Kögel-Knabner, I., Schulze, E.-D., 2013. Storage and stability of organic carbon in soils as related to depth, occlusion within aggregates, and attachment to minerals. Biogeosciences 10 (3), 1675–1691. https://doi.org/10.5194/bg-10-1675-2013.
Schwertmann, U., 1964. Differenzierung der Eisenoxide des Bodens durch Extraktion mit Ammoniumoxalat-Lösung. Zeitschrift für Pflanzenernährung, Düngung, Bodenkunde 105 (3), 194–202. https://doi.org/10.1002/jpln.3591050303.
Sokol, N.W., Sanderman, J., Bradford, M.A., 2019. Pathways of mineral-associated soil organic matter formation: integrating the role of plant carbon source, chemistry, and point of entry. Global Change Biology 25 (1), 12–24. https://doi.org/10.1111/gcb.14482.
Spielvogel, S., Prietzel, J., Kgel-Knabner, I., 2008. Soil organic matter stabilization in acidic forest soils is preferential and soil type-specific. European Journal of Soil Science 59 (4), 674–692. https://doi.org/10.1111/j.1365-2389.2008.01030.x.
Spohn, M., 2024. Preferential adsorption of nitrogen- and phosphorus-containing organic compounds to minerals in soils: a review. Soil Biology and Biochemistry 194, 109428. https://doi.org/10.1016/j.soilbio.2024.109428.
Sposito, G., 2020. The Chemistry of Soils, third ed. Oxford University Press, New York. https://doi.org/10.1093/oso/9780190630881.001.0001.
Sugai, S.F., Schimel, J.P., 1993. Decomposition and biomass incorporation of 14c-labeled glucose and phenolics in taiga forest floor: effect of substrate quality, successional state, and season. Soil Biology and Biochemistry 25 (10), 1379–1389. https://doi.org/10.1016/0038-0717(93)90052-D.
Sulman, B.N., Phillips, R.P., Oishi, A.C., Shevliakova, E., Pacala, S.W., 2014. Microbe-driven turnover offsets mineral-mediated storage of soil carbon under elevated CO2. Nature Climate Change 4 (12), 1099–1102. https://doi.org/10.1038/nclimate2436.
Tributh, H., Lagaly, G., 1986. Aufbereitung und Identifizierung von Boden- und Lagerstättentonen. I. Aufbereitung der Proben im Labor, vol. 30. GIT-Fachzeitschrift für das Laboratorium, pp. 524–529.
Uroz, S., Kelly, L.C., Turpault, M.-P., Lepleux, C., Frey-Klett, P., 2015. The mineralosphere concept: mineralogical control of the distribution and function of mineral-associated bacterial communities. Trends in Microbiology 23 (12), 751–762. https://doi.org/10.1016/j.tim.2015.10.004.
Van Veldhoven, P.P., Mannaerts, G.P., 1987. Inorganic and organic phosphate measurements in the nanomolar range. Analytical Biochemistry 161 (1), 45–48. https://doi.org/10.1016/0003-2697(87)90649-X.
Vance, E.D., Brookes, P.C., Jenkinson, D.S., 1987. An extraction method for measuring soil microbial biomass C. Soil Biology and Biochemistry 19 (6), 703–707. https://doi.org/10.1016/0038-0717(87)90052-6.
Wang, G., Post, W.M., Mayes, M.A., 2013. Development of microbial-enzyme-mediated decomposition model parameters through steady-state and dynamic analyses. Ecological Applications 23 (1), 255–272. https://doi.org/10.1890/12-0681.1.
Wickham, H., 2016. ggplot2. Springer International Publishing, Cham. https://doi.org/10.1007/978-3-319-24277-4.
Wilcoxon, F., 1945. Individual comparisons by ranking methods, 1 (No.6), 80–83.
Yeasmin, S., Singh, B., Kookana, R.S., Farrell, M., Sparks, D.L., Johnston, C.T., 2014. Influence of mineral characteristics on the retention of low molecular weight organic compounds: a batch sorption–desorption and ATR-FTIR study. Journal of Colloid and Interface Science 432, 246–257. https://doi.org/10.1016/j.jcis.2014.06.036.